A comparison between optically active CdZnSe/ZnSe and CdZnSe/ZnBeSe self-assembled quantum dots: effect of beryllium

Y. Gu[a],*, Igor L. Kuskovsky[a,1], R.D. Robinson[a], I.P. Herman[a], G.F. Neumark[a], X. Zhou[b], S.P. Guo[b], M. Munoz[b], M.C. Tamargo[b]

[a]Department of Applied Physics and Applied Mathematics, Columbia University, New York, NY 10027, USA
[b]Department of Chemistry, City College of CUNY, New York, NY 10031, USA

Abstract

The composition and size of optically active $Cd_xZn_{1-x}Se/ZnSe$ quantum dots are estimated with a previously developed method. The results are then compared with those obtained for $Cd_xZn_{1-x}Se/Zn_{0.97}Be_{0.03}Se$ QDs. We show that introducing Be into the barrier material enhances both Cd composition and quantum size effect of optically active quantum dots.
© 2005 Elsevier Ltd. All rights reserved.

1. Introduction

Self-assembled quantum dot (QD) systems have been of great interest due to their unique optical properties and easy integration into existing electronic circuits. For device applications, QDs have to have narrow distributions of size and composition. However, although with III–V system (e.g. InAs/GaAs) the formation of rather uniform QDs can be well controlled by the growth conditions, and QDs of sizes below 10 nm with very high packing densities have been obtained (Ref. [1]), it seems to be more difficult to achieve such QDs for the II–VI system (e.g. CdSe/ZnSe).

Recently Be has been introduced into the ZnSe barrier with the expectation to enhance both barrier crystalline quality and QD formation [2,3]. Moreover, it has been shown [4] that there is a Be-induced island formation in CdZnSe/ZnSe system even below critical thickness for Stranski–Krastanow growth. It would be further interesting to compare optically active CdZnSe/ZnSe and CdZnSe/ZnBeSe QDs in their properties (e.g. size and chemical composition). This is difficult to achieve with typical structural characterizations such as transmission electron microscopy (TEM), since the QDs investigated under TEM do not necessarily participate in the optical processes (optically inactive QDs).

In our previous work [5], we showed how to estimate the size and composition of optically active QDs using optical studies and model calculations. We applied this approach to $CdZnSe/Zn_{0.97}Be_{0.03}Se$ QD, and have found that the quantum dots have Cd composition (x) of ∼0.47–0.54 and diameter (d) between 5.1 and 8.0 nm [5].

In this paper, we extend such an approach to CdZnSe/ZnSe QDs grown under comparable conditions to

* Corresponding author. Address: Department of Materials Science and Engineering, Northwestern University, Evanston, IL 60208, USA. Tel.: +1 8474674680; fax: +1 2085755369.
E-mail address: yi-gu@northwestern.edu (Y. Gu).
[1] Present address: Department of Physics, Queens College of CUNY, Flushing, NY 11367, USA.

those for CdZnSe/Zn$_{0.97}$Be$_{0.03}$Se QDs studied in Ref. [5]. Thus, we give typical values of Cd composition and size of optically active CdZnSe/ZnSe QDs; compare with those obtained on CdZnSe/Zn$_{0.97}$Be$_{0.03}$Se QDs, and finally suggest the effect of beryllium on these QDs.

2. Experimental

Both samples were grown by molecular beam epitaxy (MBE) on GaAs (001) substrates in a dual chamber Riber 2300 system, which has a III–V growth chamber and a II–VI growth chamber. A 200 nm GaAs buffer layer, 30 periods of (2 nm GaAs/2 nm AlAs) short-period superlattice and a 30 nm GaAs layer were grown at 580 °C in the III–V chamber after the deoxidization of GaAs substrate under an As flux. Then the substrate with III–V buffer layers was transferred into the II–VI chamber in UHV. Prior to the growth of II–VI epilayers, a Be–Zn co-irradiation of the GaAs surface was performed at 170 °C. Then the substrate temperature was increased to 250 °C and a 6 nm ZnSe buffer layer was grown. After this Zn$_{0.97}$Be$_{0.03}$Se (or ZnSe) epilayers, which are nearly lattice-matched to GaAs, was grown at 270 °C. CdSe QDs were formed by depositing 2.5 ML of CdSe on ZnBeSe (or ZnSe) surface and with a growth interruption of 30 s.

For photoluminescence (PL) measurements, samples were excited by the 325 nm emission from a He–Cd laser. A 300 W Xenon lamp coupled to a 1/4 m monochromator was used as the excitation source for the photoluminescence excitation (PLE) experiments. The PL signal was recorded with a 3/4 m monochromator, a thermoelectrically cooled GaAs photomultiplier tube, and a photon counter. A closed cycle refrigerator system was used for low-temperature PL measurements. Polarized Raman scattering was performed with the 488 and 514.5 nm lines of an Ar$^+$ laser in the backscattering configuration with only LO phonon scattering allowed. To reduce the heating effect in the samples for Raman measurements, all incident power was kept below 1 mW. A 0.6 m triple spectrometer in subtractive configuration with a Si CCD array detector was used to record the Raman spectra.

3. Results

3.1. Photoluminescence and photoluminescence excitation

In Fig. 1 we plot low-temperature ($T = 9$ K) PL (the solid line) and PLE (circles) spectra from the CdZnSe/ZnSe QDs; the PL (the dashed line) from the CdZnSe/Zn$_{0.97}$Be$_{0.03}$Se QDs [5] is also shown for comparison. The PL spectra of both samples show a single peak at 2.39 and 2.43 eV, respectively. The specific PL energy position depends on x and size of the optically active QDs. The PLE spectrum shows a free exciton peak (2.803 eV) from the barrier
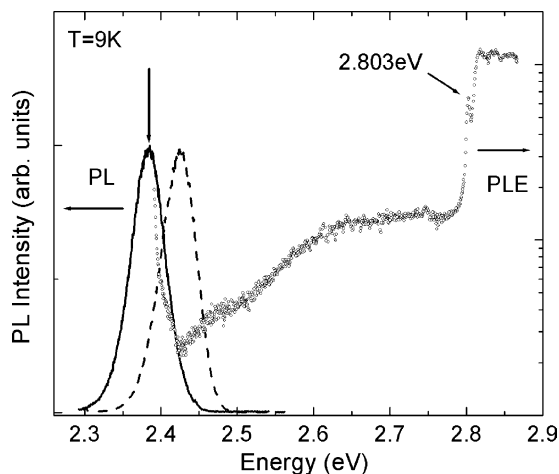

Fig. 1. PL (the solid line) and PLE (open circles) spectra of CdZnSe/ZnSe QDs; the arrow indicates the detection energy. The PL of CdZnSe/ZnBeSe QDs (the dashed line) is shown for comparison.

(ZnSe) and a broad feature associated with the excitation via the 2D ternary CdZnSe layer. No phonon-assisted excitation can be observed in CdZnSe/ZnSe QDs, in sharp contrast to the PLE spectrum from CdZnSe/ZnBeSe QDs [5], where LO and surface (SF) phonon peaks were clearly seen.

In Fig. 2 we plot the integrated PL intensity as a function of temperature, which, for the CdZnSe/ZnSe QDs (solid circles), remains relatively constant up to $T = 140$ K (indicated by the arrow), and decreases by two orders of magnitude at $T = 280$ K compared to that at $T = 9$ K. On the other hand, for CdZnSe/ZnBeSe QDs, the PL intensity
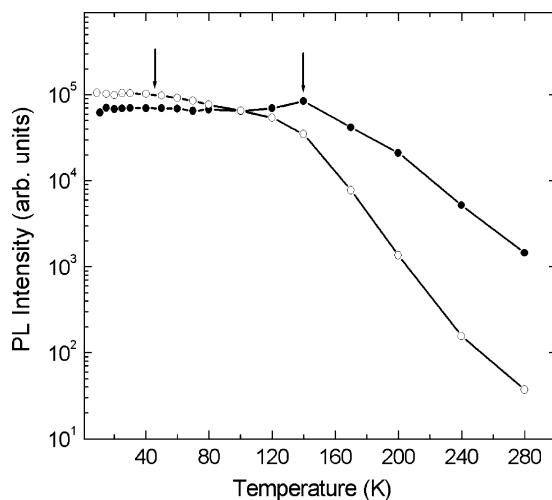

Fig. 2. The integrated PL intensity as a function of temperature for CdZnSe/ZnSe (solid circles) and CdZnSe/ZnBeSe QDs (open circles). The line is the guide for the eye. The arrows indicate the temperature up to which the PL intensity remains relatively constant.

(open circles) starts decreasing at around $T = 45$ K (indicated by the arrow), and decreases by more than three orders of magnitude at $T = 280$ K compared to that at $T = 9$ K.

3.2. Raman scattering

In Fig. 3(a) and (b) we show the room temperature (RT) Raman scattering spectra of CdZnSe/ZnSe QDs with the 488 and 514.5 nm lines of an Ar^+ laser, respectively. In relation to the QD PL spectrum (see the inset in Fig. 3(a)), they represent the non-resonant and the resonant cases, respectively. Under the 488 nm excitation, we observe the LO phonons from GaAs substrate (~ 289 cm^{-1}) and the ZnSe barrier (~ 251 cm^{-1}) as well as a small peak at around 243 cm^{-1} and a strong, quite narrow, symmetric peak at 223 cm^{-1}. To identify the origins of the latter two peaks, we first note that the contactless electroreflectance measurements performed on the same sample revealed that there is a transition at ~ 2.56 eV [6], which was attributed to the 2D ternary CdZnSe layer. This energy is quite close to the photon energy (~ 2.54 eV) corresponding to the 488 nm laser line used in this experiment. Therefore, the scattering from LO phonons in the 2D ternary CdZnSe layer will be significantly enhanced due to the resonant conditions (Ref. [7]), resulting in the strong narrow Raman response, which

we indeed have observed at 223 cm^{-1}. Thus, it seems logical to assign this peak to the LO phonons in the 2D ternary CdZnSe layer. No such a peak was observed in the CdZnSe/ZnBeSe sample [5], where, apparently, the resonant conditions were not satisfied due to the different Cd composition and/or thickness of the 2D ternary CdZnSe layer. As to the 243 cm^{-1} peak, we note that a similar peak (at ~ 244 cm^{-1}) was observed in the CdZnSe/ZnBeSe system [5], and it was attributed to LO phonons in the 2D ternary CdZnSe layer or to interface (IF) phonons. Since for the CdZnSe/ZnSe system, the 223 cm^{-1} peak is identified here as LO phonon in the 2D ternary CdZnSe layer, it follows that the 243 cm^{-1} peak is due to the IF phonons between CdSe QDs and ZnSe barriers (this coincides with the assignment given in Ref. [8]). Thus, this also allows us to assign the 244 cm^{-1} peak in the CdZnSe/ZnBeSe system [5] to the similar IF phonons.

In the Raman spectrum obtained with the 514.5 nm line (Fig. 3(b)), in addition to the GaAs and ZnSe LO phonon peaks, we observe a weak peak at 268 cm^{-1}, which we attribute to the GaAs TO phonons [7]. The IF phonon peak (246 cm^{-1}) dominates the spectrum, in contrast to what has been observed from the 488 nm case (Fig. 3(a)). Similar phenomenon has been reported for this type of structure, and is suggested to be due to the coupling between IF phonons and excitons localized in the CdZnSe QDs [9]. This also is consistent with the theory of resonant Raman scattering of spheroidal QDs (see Ref. [10] and references therein). Additionally, a relatively broad peak at around 228 cm^{-1} is observed. Since this peak appears only under the resonant conditions in relation to the QD PL, we attribute it to LO phonons in the CdZnSe QDs.

3.3. Calculations

We have shown previously how to use model calculations and available PLE and/or Raman scattering data to estimate chemical composition and the size of optically active QDs [5]. Following this approach, as the next step, we calculate the PL transition energies for QDs and the 2D ternary CdZnSe layer in the CdZnSe/ZnSe system as a function of both Cd composition and the size.

For QDs, we use the quantum disk model [11] under the condition $R \gg L_Z$, where R and L_Z are the radius and the height of the disk, respectively. Within such a model, the in-plane confinement is described by 2D harmonic potentials (see, e.g. Ref. [12] and references therein) and the vertical-plane confinement is modeled as a square well with finite potential barriers that are determined by the Cd composition of the QDs. The Coulomb interaction is usually ignored, since its contribution to the total energy is very small for the $R \gg L_Z$ condition [12]. The materials parameters are the same as those used in Ref. [5].

Within this model, we calculated the combinations of QD Cd compositions and sizes that contribute to the 2.41 eV (514 nm) PL energy, assuming R/L_Z equals 5 and 10 (dashed
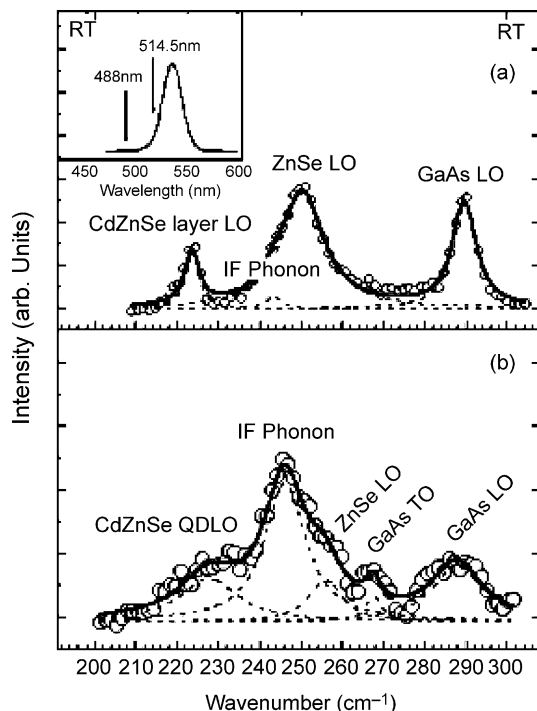

Fig. 3. The RT polarized Raman scattering spectra for CdZnSe/ZnSe QDs: (a) using the 488 nm laser line and (b) using the 514.5 nm laser line. The inset is the RT PL of the same sample. Open circles represent the experimental data, and the solid line is the result of fitting with Lorentzians (dashed lines).
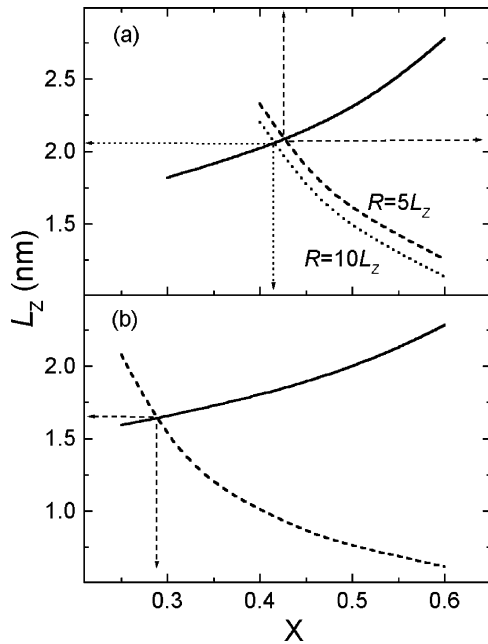
Fig. 4. The procedure for the estimation of Cd composition (x) and height (L_Z) for (a) QDs and (b) the ternary CdZnSe layer of CdZnSe/ZnSe sample. The solid lines correspond to the LO phonon energy, and the dashed and dotted lines represent the PL energy (see also text). The arrows indicate the intersections of curves.

and dotted lines in Fig. 4(a), respectively). We then also expressed the corresponding (Fig. 3(b)) QD LO phonon energy, $\hbar\omega_{LO} = 28.3$ meV (228 cm^{-1}), as a function of QD Cd composition and size, using the theory developed in Ref. [12]. The result is plotted in Fig. 4(a) as the solid line. The intersection of these curves (Fig. 4(a)) gives the composition (x) and size of QDs that emit at 2.41 eV. We note that, for different R/L_Z ratios, the results are almost identical: $x = 0.43$, $L_Z = 2.1$ nm for $R/L_Z = 5$, and $x = 0.42$, $L_Z = 2.1$ nm for $R/L_Z = 10$.

The same procedure was carried out for the 2D ternary CdZnSe layer (Fig. 4(b)) using the PL energy (2.54 eV) that corresponds to 488 nm (see Fig. 3(a)) and $\hbar\omega_{LO} = 27.6$ meV (223 cm^{-1}). We modeled the 2D ternary CdZnSe layer as a square well with finite barriers, and we obtained $x = 0.29$ and $L_Z = 1.6$ nm. These can be compared to transmission electron microscopy (TEM) studies on similar structures, which showed that the x of the 2D ternary CdZnSe layer ranges from 0.21 [13] to 0.35 [14], with the height ~ 10 ML [13,14] (~ 2.8 nm), in reasonable agreement with our results.

4. Discussion

Ideally, to determine the effect of Be on the Cd composition and size of optically active QDs, one should

apply the procedure described above at various energies across the CdZnSe/ZnSe QD PL (as has been done in Ref. [5] for the CdZnSe/ZnBeSe system), which requires the knowledge of LO phonon energy at any specific PL energy. Unfortunately, unlike in the case described in Ref. [5], we did not observe phonon peaks in PLE (Fig. 1) spectrum of CdZnSe/ZnSe QDs, suggesting a relatively weaker exciton–phonon coupling. The strength of exciton–phonon coupling decreases with decreasing Cd composition and/or increasing QD size (above some critical size) [15]. Therefore, we conclude that the optically active CdZnSe/ZnSe QDs have lower Cd compositions and/or they are larger than the CdZnSe/ZnBeSe QDs.

It must be further noted that for CdZnSe/ZnBeSe QDs the high energy side of the PL is dominated by QDs with smaller sizes and higher Cd compositions [5]. Thus, assuming a similar trend for $Cd_xZn_{1-x}Se/ZnSe$ QDs, the values of $x = 0.42$–0.43 obtained above represent the high limit of the Cd composition in CdZnSe/ZnSe QDs, which is notably lower than any x (0.47–0.54) obtained for CdZnSe/ZnBeSe QDs [5], which is consistent with the lack of phonon-related peaks in the PLE. Therefore, we suggest that the addition of Be into the barriers enhances Cd compositions of optically active QDs [16].

As to the QD size only a comparison in the overall quantum size effect can be made. We consider the following arguments. The PL peak energy of CdZnSe/ZnBeSe QDs is higher by ~ 40 meV than that of CdZnSe/ZnSe QDs (Fig. 1), and such a difference cannot be accounted for by the change in the barrier height caused by the addition of Be, since within the same model (sphere or disk), the calculated difference in the PL energy resulting from the increased barrier height (by ~ 66 meV), is only ~ 2 meV. Moreover, higher Cd compositions in CdZnSe/ZnBeSe QDs would lead to the narrower bandgap and thus lower PL energies. Therefore, one would expect the CdZnSe/ZnBeSe QD PL at the lower energies than that of CdZnSe/ZnSe QDs if both systems were characterized by the same quantum size effect. Here we, however, observe the opposite, which suggests that the presence of Be leads to stronger quantum size effect. This conclusion is further confirmed by the comparison of the PL temperature behaviors of both samples (Fig. 2). Indeed, the weaker PL of CdZnSe/ZnBeSe QDs at high temperatures suggests weaker exciton localizations, which result from higher-lying quantization levels (shallower levels), consistent with stronger quantum size effects. This enhanced quantum size effect most likely results from the reduction of the QD lateral size, since the previous time-resolved photoluminescence measurements [17] suggest a 3D quantum confinement for the CdZnSe/ZnBeSe quantum dots.

5. Conclusions

In conclusion, we have estimated, for the first time, the

Cd composition and size of optically active CdZnSe/ZnSe QDs using Raman scattering and PL spectroscopies, complemented by model calculations. This allows for the comparison between the properties of CdZnSe QDs embedded in ZnSe and ZnBeSe matrixes. Such a comparison suggests that introduction of Be into ZnSe matrix enhances both Cd composition and overall quantum size effects of optically active CdZnSe QDs.

References

[1] G.S. Solomon, J.A. Trezza, J.S. Harris, J. Appl. Phys. 66 (1995) 991.
[2] M. Keim, M. Korn, J. Seufert, G. Bacher, A. Forchel, G. Landwehr, S. Ivanov, S. Sorokin, A.A. Sitnikova, T.V. Shubina, A. Toropov, A. Waag, J. Appl. Phys. 88 (2000) 7051.
[3] S.P. Guo, X. Zhou, O. Maksimov, M.C. Tamargo, C. Chi, A. Couzis, C. Maldarelli, I.L. Kuskovsky, G.F. Neumark, J. Vac. Sci. Technol. B 19 (2001) 1635.
[4] J. Seufert, M. Rambach, G. Bacher, A. Forchel, M. Keim, S. Ivanov, A. Waag, G. Landwehr, Phys. Rev. B 62 (2000) 12609.
[5] Y. Gu, I.L. Kuskovsky, J. Fung, R. Robinson, I.P. Herman, G.F. Neumark, X. Zhou, S.P. Guo, M.C. Tamargo, Appl. Phys. Lett. 83 (2003) 3779.
[6] M. Munoz, S.P. Guo, X. Zhou, M.C. Tamargo, Y.S. Huang, C. Trallero-Giner, A.H. Rodriguez, Appl. Phys. Lett. 83 (2003) 4399.
[7] P.Y. Yu, M. Cardona, Fundamentals of Semiconductors, second ed., Springer, Berlin, 1999.
[8] H. Rho, H.E. Jackson, S. Lee, M. Dobrowolska, J.K. Furdyna, Phys. Rev. B 61 (2000) 15641.
[9] H. Rho, L.M. Smith, H.E. Jackson, S. Lee, M. Dobrowolska, J.K. Furdyna, Phys. Status Solidi B 224 (2001) 165.
[10] C. Trallero-Giner, Phys. Status Solidi B 241 (2004) 572.
[11] Previous time-resolved PL studies on the same sample (X. Zhou, M.C. Tamargo, S.P. Guo, Y.C. Chen, J. Electron. Mater. 32 (2003) 733) show that the PL decay time increases linearly with temperature, indicating a quasi-two-dimensional character (quantum disk).
[12] E. Menendez-Proupin, C. Trallero-Giner, S.E. Ulloa, Phys. Rev. B 60 (1999) 16747.
[13] D. Litvinov, D. Gerthsen, A. Rosenauer, H. Preis, E. Kurtz, C. Klingshirn, Phys. Status Solidi B 224 (2001) 147.
[14] N. Peranio, A. Rosenauer, D. Gerthsen, S.V. Sorokin, I.V. Sedova, S.V. Ivanov, Phys. Rev. B 61 (2000) 16015.
[15] D.V. Melnikov, W.B. Fowler, Phys. Rev. B 64 (2001) 245320.
[16] We understand that the actual values for L_Z and x depend on the material parameters used for calculations; however, since the accuracy of these material parameters for ZnSe and ZnBeSe is expected to be similar, this comparison remains valid.
[17] X. Zhou, M.C. Tamargo, S.P. Guo, Y.C. Chen, J. Electron. Mater. 32 (2003) 733.